Available online at www.sciencedirect.com
SCIENCE DIRECT
Polymer 47 (2006) 3935–3945
polymer
www.elsevier.com/locate/polymer

Non-isothermal crystallization and thermal transitions of a biodegradable, partially hydrolyzed poly(vinyl alcohol)

He Huang [a,b,*], Lixia Gu [b], Yukihiro Ozaki [a,*]

[a] Department of Chemistry, School of Science and Technology and Research Center for Environmental Friendly Polymers, Kwansei-Gakuin University, Gakuen, Sanda 669-1337, Japan
[b] College of Materials Science and Engineering, Donghua University, Shanghai 200051, China.

Received 1 December 2005; received in revised form 21 March 2006; accepted 25 March 2006
Available online 18 April 2006

Abstract

A study has been made of the non-isothermal crystallization behavior and thermal transitions of a biodegradable, partially hydrolyzed poly(vinyl alcohol) with 80% degree of saponification (PVA80). Possible sample degradation was first investigated, but no significant degradation or dehydration was detected using FTIR and DSC under the experimental condition. The non-isothermal crystallization of PVA80 was analyzed with Ozawa equation, and the Mo method of combining Ozawa and Avrami equations. Ozawa equation was only applicable in a narrow temperature range from 80 to 100 °C. The deviation from the Ozawa equation is not due to the secondary crystallization or the quasi-isothermal nature of the treatment. It is only a result of the large relative difference of the relative crystallinity values under different cooling rates. The Mo method demonstrated a success in the full temperature range investigated. The isoconversional method developed by Friedman failed to estimate the activation energy for this non-isothermal crystallization. Thermal transitions of PVA80 are associated with its complex hydrogen-bonding interactions. The melt-crystallized PVA80 sample, as that from film casting, followed by annealing at 60 and 80 °C, has a broad melting temperature range measured by DSC and FTIR. It was found that the melting behavior of a semicrystalline polymer can be probed via a non-crystalline hydrogen-bonded C=O band using FTIR. The glass transition temperature T_g of PVA80 was raised about 20 °C, after the sample was melt-crystallized. The intensity of the hydrogen-bonded C=O band increases when temperature was increased from 110 to 180 °C, due to the promoted hydrogen-bonding interactions between the C=O groups in the amorphous phase and the hydroxyl groups from the crystalline phase, which is also the main reason for the increased T_g transition.

Keywords: Partially hydrolyzed poly(vinyl alcohol); Non-isothermal crystallization; Thermal transitions

1. Introduction

Poly(vinyl alcohol) (PVA) is an important water-soluble polymer which has vast industrial applications, such as in fibers, textile sizing and finishing agents, coatings, adhesives, emulsifiers, colloidal stabilizers, and building industry, etc. [1–3]. PVA has also found its application as a barrier film for food packaging [4], because PVA has excellent gas barrier property due to small, dense, and closely packed 'Monoclinic' crystallites [4–6], as well as flexibility, transparency and toughness, etc. It is very unique that even an atactic-PVA is semi-crystalline despite of its lack of steroregularity [5–7]. In addition, high strength fibers can be produced when PVA is filled with nanotubes [8–12]. For example, Baughman et al. [12] demonstrated that high nanotube content fibers made with PVA have a tensile strength half that of Kevlar®, and a toughness 15 times of Kevlar® and three times that of spider silk, though PVA is not a good candidate for the continuous phase of a polymer composite, because of its extreme water sensitivity, susceptibility to thermal degradation, and relatively high glass transition temperature. Furthermore, PVA is also known to be biodegradable [13,14], which offers PVA another important application as biomaterials, including biodegradable poly(vinyl alcohol) based blend materials [14]. Among them, poly(3-hydroxybutyrate) (PHB)/PVA blends [15–20] are the ones we are interested in so far.

When PVA is blended with PHB, one problem appears, however; the DSC melting peak of PVA is severely overlapped with the thermal decomposition peak of PHB [16]. This problem

* Corresponding authors. Address: Department of Chemistry, School of Science and Technology and Research Center for Environmental Friendly Polymers, Kwansei-Gakuin University, Gakuen, Sanda 669-1337, Japan. Tel.: +81 79 565 8354; fax: +81 79 565 9077.
E-mail addresses: h99huang@yahoo.com (H. Huang), ozaki@ksc.kwansei.ac.jp (Y. Ozaki).

0032-3861/$ - see front matter © 2006 Elsevier Ltd. All rights reserved.
doi:10.1016/j.polymer.2006.03.089

makes it difficult to observe the thermal behavior and morphological properties of PVA in the blends, such as its crystallinity by DSC. A partially hydrolyzed PVA with a saponification degree of 78–82% (thereafter called PVA80 for the sake of convenience), which is also biodegradable [14], has a much lower melting point [21] (ca. 180 °C), which is slightly higher than that of PHB. Therefore, it becomes feasible now to observe the thermal behavior and morphological properties of PVA80 in the blends with PHB [21], which makes PVA80 a good candidate for a biodegradable blend partner for PHB, when the blends are designed for biodegradable materials.

In a previous paper [21], we reported the miscibility and hydrogen bonding interactions, as well as the morphological properties of PVA80 and PHB in PHB/PVA80 blends. Due to the semi-crystalline nature of both PVA80 and PHB, it is naturally important to investigate the melting and crystallization behaviors of PHB, PVA80 and their blends. In fact, the melting and crystallization of semi-crystalline polymers has long been one of the most heavily studied areas in the field of polymer science [22–26]. The melting and crystallization behaviors of PHB have been studied intensively in the past [27–33]. In the literature, however, there was a lack of studies on the crystallization kinetics of PVA [34], needless to say PVA80, in the absence of solvent or plasticizer, because this polymer degrades at temperatures near its melting temperature. This is the reason that products of PVA films have been mainly produced by wet or gel spinning and coating. Melt processing, such as melt spinning and injection molding, has been impractical due to serious thermal degradation in the melt of PVA. It would be a tremendous development if melt processing was possible, which would lead to environmental-friendly operation, higher productivity rate in manufacturing, and increase in PVA products, as well as increase of physical properties, etc. Recently, fibers with high modulus and high strength have been made from partially saponificated PVA via gel spinning [35,36]. Naturally, there is a demand to have a detailed study on the thermal properties and crystallization behaviors of partially hydrolyzed PVA.

It is well known that PVA has a strong tendency to exhibit inter- and intra-molecular hydrogen bonds. In PVA80, the hydrogen bonding interaction is more complicated by the incorporation of vinyl acetate units on the molecular chain. Therefore, it is not only necessary but also interesting to investigate the thermal and crystallization behaviors of PVA80, because it possesses separate and interesting issues. In this report, the non-isothermal crystallization behavior and thermal transitions of PVA80 were studied by using FTIR and DSC. Prior to that, possible sample degradation was first investigated, due to its importance associated with the crystallization and thermal transitions.

2. Experimental

2.1. Materials

Partially hydrolyzed PVA ($T_m \sim 180$ °C) sample with a saponification degree of 78–82% (PVA80) and degree of polymerization of 2000, was purchased from Wako Co., Japan. 1,1,1,3,3,3-hexafluoisopropanol (HFIP) was used as solvent, which was also purchased from Wako Co., Japan.

2.2. DSC measurement

All DSC measurements were performed on a Perkin–Elmer Pyris 6 apparatus, under a nitrogen purge. Sample weights were about 4–7 mg, and they were used as received.

For non-isothermal crystallization experiments, PVA80 samples were heated from 30 to 200 °C with a heating rate of 10 °C/min, where the samples were kept for 2 min. Then, the samples were cooled to 30 °C at constant rates of 2, 5, 10, 20 and 40 °C/min, respectively.

2.3. Fourier transform infrared measurement

Thin films of PVA80 were prepared by casting from solutions of 1,1,1,3,3,3-hexafluoisopropanol (HFIP). All the thin film were left in air for 1 day, and dried in a vacuum oven at 60 °C for 1 day and then 80 °C for another day. The samples made were kept in a dessicator at room temperature until use.

Infrared spectra were obtained on a Thermo Nicolet NEXUS Fourier transform infrared (FTIR) spectrometer using a minimum of 128 co-added scans at a resolution of $2\ cm^{-1}$. The film was sufficiently thin to be within the absorbance range where the Beer–Lambert law is obeyed. The temperature of the sample cell was controlled with a thermoelectric device (CN4400, OMEGA) with an accuracy of ± 0.2 °C.

3. Results and discussion

3.1. Probing possible degradation of PVA80 during non-isothermal crystallization

As mentioned in Section 1, PVA degrades at its melting temperature, which leads to the paucity of studies on the crystallization kinetics of PVA [34]. Nevertheless, Peppas et al. [37] investigated the kinetics and mechanisms of crystallization of PVA in the solvent-free state under isothermal conditions. The possible degradation or dehydration of the PVA samples in the range of experimental conditions was judged by comparing IR spectra before and after crystallization at high temperature (192 °C). It was concluded that there was no evidence for degradation, dehydration or related reactions. This, however, was questioned by Probst et al. [34], who argued that IR spectroscopy is much less sensitive than the method they used, namely repeatability of DSC measurements. A recent study by Endo et al. [38] claimed to have found conditions that allow studying melt crystallization of PVA without thermal degradation. The process involves degassing the film using a diffusion pump at room temperature for several hours, followed by thermal treatments being performed under this same vacuum. The possible degradation of PVA samples was judged by changes in the polydispersity index. This was questioned again by Probst et al. [34] who insisted that

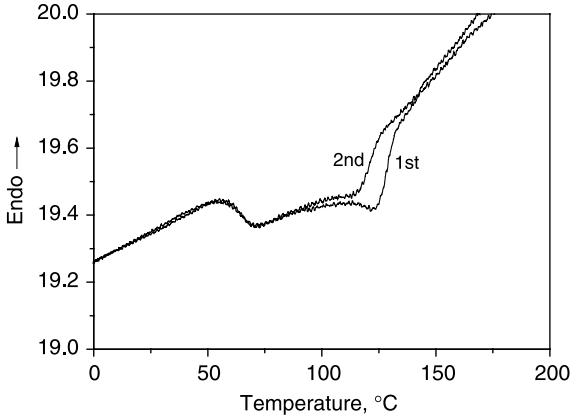

Fig. 1. DSC thermograms of PVA80 on the first and second cooling scans (cooling rate, 2 °C/min).

polydispersity index is not a very sensitive method. Besides, they argued that crystallization kinetics cannot be measured using this approach because a DSC cell cannot be maintained under such a high vacuum [34]. However, the method that Probst et al. [34] suggested, namely repeatability of DSC measurements is not a direct way to detect degradation in the crystallization process, because this will require to run a sample under the experimental conditions for another time. More specifically, even if there is no degradation on the first run, sample degradation might happen on the second run due to the double time of remaining in the heating cell.

Nevertheless, as an extreme example, Fig. 1 shows DSC thermograms of PVA80 on the first and second cooling scans at the lowest cooling rate of 2 °C/min. In this case, the PVA80 sample was kept in the heating cell at high temperature for the longest time. Though the shift of the crystallization temperature to a lower one and a lowering of the heat release associated with crystallization, both effects attributed to sample degradation, were observed, the situation of sample degradation is not so serious as in the non-isothermal crystallization experiments performed on PVA mixed with single-walled carbon nanotubes, as reported by Probst et al. [34], where carbon nanotubes promoted the thermal degradation of PVA. Besides, the T_g values of PVA on the first and second cooling scans are completely identical, suggesting that no significant degradation happened. To reiterate, lower temperature shift of the crystallization temperature and a lowering of the heat release on the second cooling run are not direct evidences that a sample degrades on the first cooling run.

It turns out that IR spectroscopy may still be a more direct way to detect possible degradation in the crystallization process, because the real situation of a sample in the DSC cell may be copied in an IR spectrometer. In fact, IR spectroscopy has long been a routine way to monitor possible sample degradation under heating. Fig. 2 shows the IR spectra of PVA80 taken at room temperature before and after the sample was heated to 200 °C at 2 °C/min, where the sample was first kept for 2 min, corresponding to the DSC measurement at a heating rate of 2 °C/min, then automatically cooled down to room temperature. The major observable changes include the lowering of absorbance, the slightly higher wavenumber shift of the H–O stretching band, and the weakening of the crystalline band around 1144 cm^{-1} [3], after the sample was heated to 200 °C. The lowering of

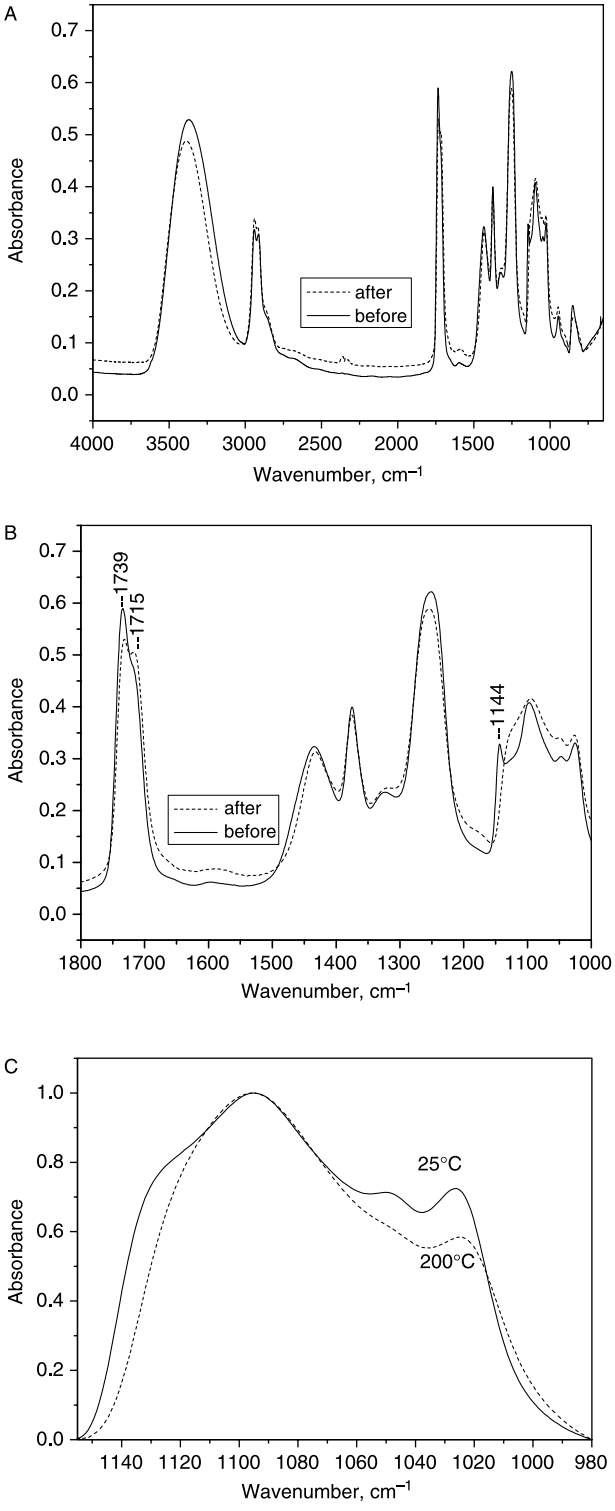

Fig. 2. IR spectra of PVA80 at room temperature before and after it was heated at 2 °C/min to 200 °C in air flow: (A) in the range of 4000–700 cm^{-1}; (B) in the range of 1800–1000 cm^{-1}. Shown in (C) are two scale-expanded spectra in the range of 1170–980 cm^{-1} taken at 200 and 25 °C when the sample was cooled from 200 to 25 °C.

absorbance is obviously a result of film thinning due to thermal expansion and even sample flow at high temperature. The slightly higher wavenumber shift of the hydroxyl peak arises from the weakening of hydrogen bonds, more specifically the formation of hydrogen bonds between the C=O groups of vinyl acetate units and the hydroxyl groups of vinyl alcohol units, due to the melting of crystallites. This can be easily verified by the relative intensity change of the 'free' C=O band at 1739 cm^{-1} and the hydrogen-bonded C=O band at 1715 cm^{-1}, as shown in Fig. 2(B). It should be noted that the above IR spectra were collected in airflow. Nevertheless, no new bands were observed in Fig. 2, suggesting that no evidence for significant degradation or dehydration can be found. Considering the nitrogen flow in the DSC cell, it can be speculated that the degradation of PVA80 samples in DSC measurement is negligible.

Compared to the intensity and band shape before thermal treatment, one may notice that the band around 1144 cm^{-1} after thermal treatment seems to disappear and suggest the occurrence of thermal degradation of the sample. This is not true, however. Fig. 2(C) clearly indicates that, after cooling from 200 °C to room temperature, the intensity of the crystalline band around 1144 cm^{-1} increases, though it does not reach the same intensity before the thermal treatment (Fig. 2(B)), which is obviously a result of different thermal history of the sample.

Further considering the highest temperature, 200 °C, used in all the PVA80 DSC measurements here, which is 30 or 50 °C lower than in the isothermal crystallization of PVA [37,38], it is safe to say that the sample degradation is not so serious that it would change the main conclusions of this study, though minor degradation of PVA80 might occur under some of the experimental conditions, especially when the cooling rate is as slow as 2 °C/min.

3.2. Non-isothermal crystallization

As mentioned above, the isothermal crystallization behavior of PVA have been investigated [37,38], though the oxidation of the sample is unavoidable. In practice, however, non-isothermal crystallization, especially the non-isothermal melt-crystallization is more common and important in, for example, extrusion, moulding and film forming etc. Fig. 3 shows the crystallization exotherms of PVA80 under different cooling rates. The peak temperature T_p, and crystallization enthalpy ΔH_c are listed in Table 1. The peak temperature T_p shifts to a lower temperature as the increase of cooling rate, which is common in semi-crystalline polymers. This is explained as at a higher cooling rate, the motion and rearrangement of PVA80 molecules are not fast enough to form the necessary nuclei for its crystallization, compared to the corresponding temperature at a lower cooling rate, where a specimen can stay at each temperature for a longer time. This can also explain why the crystallization enthalpy ΔH_c decreases with increasing cooling rate, though the difference is not so significant above 10 °C/min. The above result further suggests that the non-isothermal crystallization behavior of PVA80 is controlled by nucleation process.

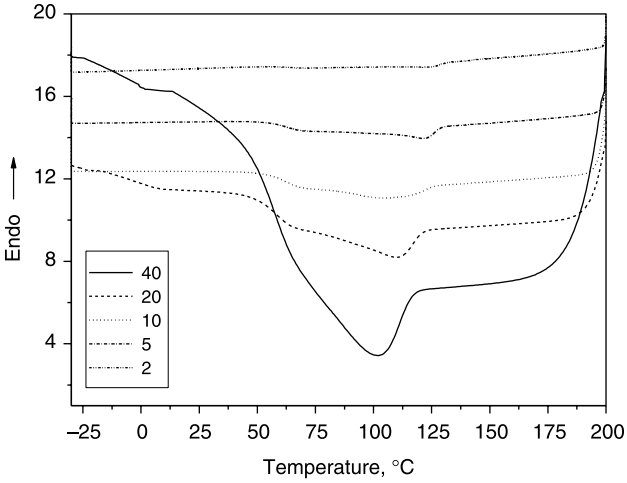

Fig. 3. Crystallization exotherms of PVA80 samples under different cooling rates (°C/min).

From the variations in the peak temperature with different cooling/heating rates ϕ, the activation energy E of the non-isothermal crystallization was usually obtained from the Kissinger method (1) [39,40]

$$d[\ln(\phi/T_p^2)]/d(1/T_p) = -E/R \quad (1)$$

where R is the universal gas constant. Plotting $\ln(\phi/T_p^2)$ vs. $1/T_p$ should give a straight line.

It is of note that, the above approach of estimating the activation energy has recently been questioned by Vyazovkin [41], who argued that the Kissinger equation is generally inapplicable for evaluating the activation energy of the processes that occur on cooling. Two other approaches, based on the isoconversional methods developed by Friedman [42] and by Vyazovkin [43–45] have, therefore, been suggested. These two approaches are mathematically vigorous. Nevertheless, huge difference, about 60–70 kJ/mol, was found to the activation energies of non-isothermally crystallized poly(ethylene terephthalate) (PET) obtained by the Vyazovkin method, when compared to results obtained by temperature modulated DSC [45]. Therefore, we attempted to evaluate the activation energy of PVA80 non-isothermal crystallization using the Friedman method [42,46], as shown in Eq. (2)

$$\ln(dX_t/dt) = \ln(Af(X_t)) - E/RT \quad (2)$$

Table 1
Peak temperature T_p, and crystallization enthalpy ΔH_c of PVA80 samples under different cooling rates

ϕ (°C/min)	T_p (°C)	ΔH_c (J/g)
2	123.6	−26.677
5	121.3	−23.177
10	115.1	−17.726
20	110.1	−16.950
40	102.3	−17.095

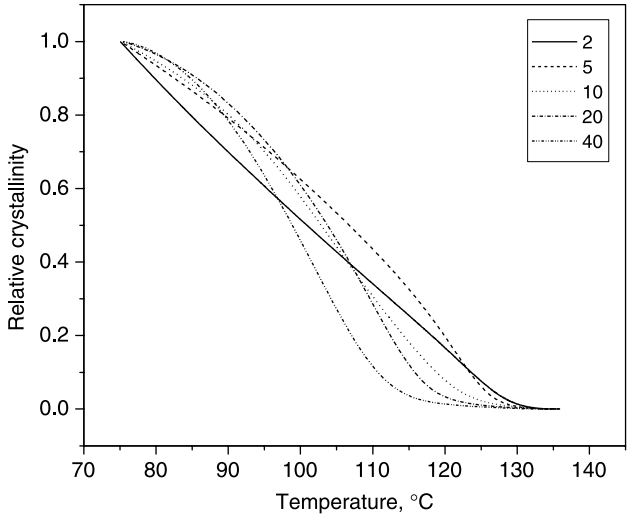

Fig. 4. Relative degree of crystallinity as a function of temperature under different cooling rates (°C/min).

where X_t is the relative degree of crystallinity, t is the time, A is the pre-exponential factor, and $f(X_t)$ is the crystallization model.

Friedman method does not work here, however, because the $\ln(dX_t/dt) \sim 1/T$ plot does not always give a straight line (not shown) at a certain value of X_t, as it is supposed to be. One of the problems is that the variation of temperature T to arrive at a certain value of X_t under different cooling rates may not be a monotonic change with cooling rate.

Integration of the exothermic peaks during the non-isothermal scans in Fig. 3 gives relative degree of crystallinity as a function of temperature. It is of note that the exothermic peaks emerge into the glass transition temperature. Thus, it is hard to determine the exact end point of an exothermic peak. We, therefore, choose the temperature range from 135 to 75 °C. Choosing 75 °C as the end point is rationalized by the fact that at this point it has roughly the same baseline as the start temperature (Fig. 3). In fact, minor variation of this end point will not change the overall trend of enthalpy values. It can also be easily shown that minor variation of start/end point of an exothermic peak will not change the overall trend of relative crystallinity vs. temperature curves. The result is shown in Fig. 4.

It can be seen from Fig. 4 that when the cooling rate is below 10 °C/min, the plots of relative crystallinity vs. temperature do not have the same sigmoid pattern as in the cases of higher cooling rates. When the cooling rate reaches 2 °C/min, the relative crystallinity changes almost linearly with temperature. The above observations imply that, not as in many other polymer systems, such as PEEKK [47] and PHB [40], etc. the retardation effect of cooling rate is not the only factor that affects the crystallization.

During a non-isothermal crystallization process, the relationship between crystallization time t and temperature T is given by Eq. (3)

$$t = |T - T_0|/\phi \tag{3}$$

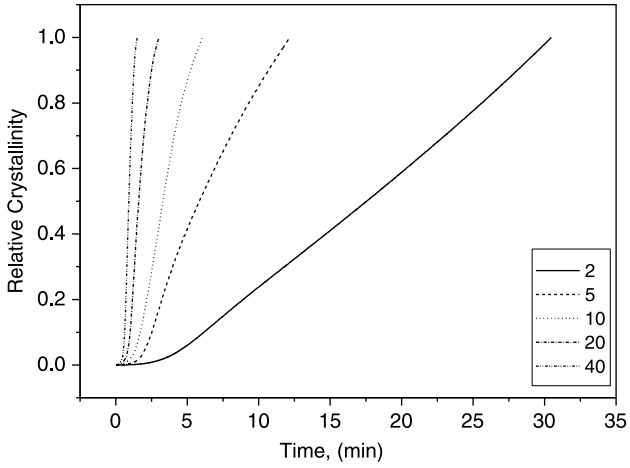

Fig. 5. Relative degree of crystallinity as a function of time under different cooling rates (°C/min).

where T is the crystallization temperature at crystallization time t, T_0 is the initial crystallization temperature at which crystallization starts, i.e. $t=0$. Based on Eq. (3), the temperature axis in Fig. 4 could be transformed into time scale, as shown in Fig. 5, where we can see the retardation effect of cooling rate, a result of rate-dependant induction time preceding the initiation of crystallization. In addition, it can be seen that the higher the cooling rate, the shorter time for the completion of crystallization. Furthermore, the plots of relative crystallinity vs. time are almost linear after the induction period, demonstrating a weak tendency of secondary crystallization, which supports the argument by Lopez and Wilkens [48], and also suggests that the widely used Ozawa equation [49] may be applicable to describe the non-isothermal crystallization process of PVA80, because secondary crystallization was not considered in this treatment [23,49].

Ozawa Eq. (4) [49] is an extension of the Avrami equation to the non-isothermal condition, by assuming that non-isothermal crystallization process may be composed of infinitesimally small isothermal crystallization steps

$$1 - X_t = \exp[-K(T)/\phi^m] \tag{4}$$

where $K(T)$ is the cooling/heating function, ϕ is the cooling/heating rate and m is the Ozawa exponent that depends on the dimension of the crystal growth.

Eq. (4) can be rearranged into Eq. (5)

$$\ln(1 - X_t) = -K(T)/\phi^m \tag{5}$$

or

$$\log(-\ln(1 - X_t)) = \log(K(T)) - m \log \phi \tag{6}$$

then, plotting $\log(-\ln(1-X_t))$ vs. $\log \phi$ at temperature T will give a straight line if the Ozawa equation is applicable, and $K(T)$ and m can be determined from the intercept and slope, respectively. The result is shown in Fig. 6.

It is apparent from Fig. 6 that Ozawa equation fails to describe the non-isothermal crystallization of PVA80 in the whole temperature range investigated, as in some other systems, such as PEEKK [47], PHB [40], poly(ether ether

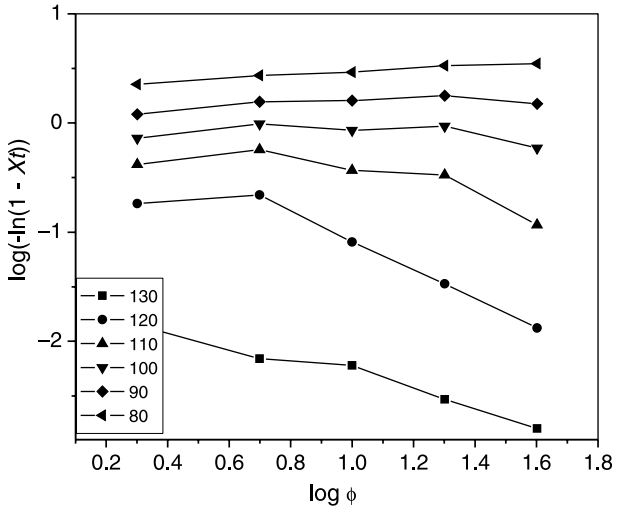

Fig. 6. Logarithmic plots of relative degree of crystallinity vs. cooling rate.

ketone) (PEEK) [50] and PE [51], etc. The reason for the failure of applying the Ozawa model has been attributed to the secondary kinetic processes in PEEKK [47], PEEK [50] and PE [51], etc. In the non-isothermal crystallization of PHB [40], however, PHB has a significantly large fraction of crystallization developing in the primary process. So, it was thought that one probable reason for the failure of applying the Ozawa model to the crystallization of PHB could be the quasi-isothermal nature of the treatment, i.e. X_t values chosen at a given temperature include the values selected from the early stage of crystallization at high heating or cooling rate and the values from the end stage at lower rate. And the crystallization kinetics was considered to be very different at low and high relative crystallization.

In the PVA80 system studied here the quasi-isothermal nature of the treatment is not the reason for the failure of applying the Ozawa model, because the difference between the maximum and minimum X_t values at each crystallization temperature under different cooling rates (Table 2), do not reflect the huge difference between the early stage of crystallization at high cooling rate and the end stage at lower rate. At 130 °C, for example, the maximum X_t is about 1.4% when the cooling rate is 2 °C/min, and the minimum X_t is about 0.16% when the cooling rate is 40 °C/min. They are both on the very beginning of crystallization. However, plotting $\log(-\ln(1-X_t))$ vs. $\log \phi$ at 130 °C does not give a parallel straight line as at 80 or 90 °C (Fig. 6).

Table 2
Relative crystallinity at temperature T under different cooling rates

ϕ (°C/min)	Relative crystallinity at temperature T (°C)					
	130	120	110	100	90	80
2	0.014	0.167	0.342	0.516	0.699	0.896
5	0.007	0.197	0.435	0.625	0.791	0.935
10	0.006	0.078	0.308	0.576	0.799	0.946
20	0.003	0.033	0.284	0.607	0.831	0.965
40	0.002	0.013	0.110	0.446	0.776	0.970
(Max − Min)/Max	0.887	0.933	0.747	0.287	0.066	0.076

Max/Min is the maximum/minimum value of relative crystallinity X_t at temperature T (°C) under different cooling rates.

Secondary crystallization is not the reason for the failure of applying the Ozawa model to PVA80 either, as already mentioned above. At 120 °C, for example, the maximum value of X_t is less than 20%, i.e. it is at the early stage of crystallization. In other words, there is no secondary crystallization at 120 °C. But plotting $\log(-\ln(1-X_t))$ vs. $\log \phi$ at 120 °C does not give a straight line. At 80 °C, however, almost all the X_t values are larger than 90%, and the maximum value of X_t is around 97% when the cooling rate is 40 °C/min, indicating the nearly completion of crystallization, where the secondary crystallization normally occurs. But $\log(-\ln(1-X_t))$ vs. $\log \phi$ at 80 °C has very good linearity. In fact, if we take a closer look at Fig. 6, it can be observed that the significant deviation from the Ozawa model starts from 110 °C, where no secondary crystallization should occur (Table 2). These suggest that there must be some other reason(s) behind this behavior.

At the bottom of Table 2, the relative difference between the maximum and minimum values of relative crystallinity X_t, i.e. (Max − Min)/Max, under each crystallization temperature is calculated. From the (Max − Min)/Max values, it is evident that it is the large relative difference of the relative crystallinity X_t values under different cooling rates that gave rise to the non-linearity between $\log(-\ln(1-X_t))$ and $\log \phi$. It is just a matter of cooling rate dependent crystallization. It also can be seen that, when the value of (Max − Min)/Max is below 30%, i.e. at the temperature range of 80–100 °C (Fig. 6), the linearity of $\log(-\ln(1-X_t)) \sim \log \phi$ is fairly good. In other words, the temperature range over which the Ozawa equation can be applied is in a narrow range, say 80–100 °C, though it does not work in the whole temperature range investigated.

A new method was developed by Mo et al. [47,52] to describe the non-isothermal crystallization process, via the combination of the Avrami and Ozawa equations.

Avrami equation

$$X_t = 1 - \exp(-kt^n) \tag{7}$$

can be rearranged as

$$\log(-\ln(1-Xt)) = \log k + n \log t \tag{8}$$

Comparing with Ozawa Eq. (6), the right-hand sides of Eqs. (6) and (8) were taken to be equal at a certain relative crystallinity X_t and crystallization time t or temperature T, for the same system investigated, i.e.

$$\log k + n \log t = \log(K(T)) - m \log \phi \tag{9}$$

or

$$\log \phi = \log(F(T)) - a \log t \tag{10}$$

where $F(T) = [K(T)/k]^{1/m}$, referring to the value of cooling/heating rate, which must be chosen at the unit crystallization time when the measured system amounts to a certain value of X_t; a is the ratio of the Avrami exponent n to the Ozawa exponent m, i.e. $a = n/m$. $\log \phi$ vs. $\log t$ plots should be linear,

Table 3
Time (min) to reach a certain X_t under a given cooling rate

ϕ (°C)	Time (min) to reach a certain X_t (%)				
	10	30	50	70	90
2	6.177	11.792	17.542	23.012	28.092
5	2.513	3.980	5.848	8.064	10.697
10	1.699	2.566	3.299	4.082	5.216
20	1.001	1.300	1.601	1.967	2.501
40	0.613	0.7807	0.913	1.063	1.263

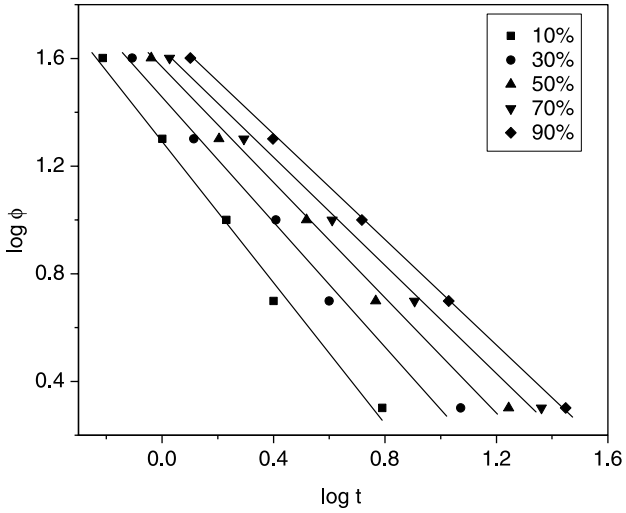

Fig. 7. Logarithmic plots of cooling rate vs. time for the non-isothermal crystallization of PVA80.

and a and $F(T)$ can be obtained from the slope and intercept of such a straight line.

Table 3 lists the time to reach a certain X_t under a given cooling rate. The $\log \phi$ vs. $\log t$ plots based on the data in Table 3, are shown in Fig. 7. A series of almost parallel lines are obtained, indicating the successful application of this approach of combination on the non-isothermal crystallization of PVA80, as PEEKK [47], PHB [40] and syndiotactic-1,2-polybutadiene (st-1,2-PB) [53].

From the straight lines in Fig. 7, a and $F(T)$ can be calculated and are listed in Table 4. It shows that $F(T)$ increases systematically with the increase of X_t, as also observed in PEEKK [47], PHB [40] and st-1,2-PB [53]. a, however, decreases with the increase of X_t, then levels off above 50%, which is different from the findings in PEEKK [47], PHB [40] and st-1,2-PB [53], where a is almost a constant. The systematic increase of $F(T)$ with X_t may be interpreted [53] as, to obtain a higher value of X_t at the unit crystallization time, a higher ϕ is required. $F(T)$ was also considered as a parameter that indicates the crystallization rate of a polymer. A lower

Table 4
Non-isothermal crystallization kinetic parameters of PVA80 at different relative crystallinity obtained by the combination of Avrami and Ozawa equations

X_t	10	30	50	70	90
$F(T)$	19.88	27.77	33.67	40.05	49.23
a	1.32	1.11	1.01	0.97	0.96

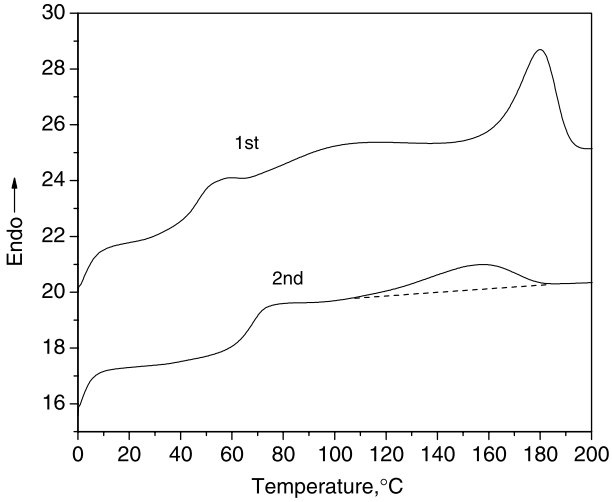

Fig. 8. DSC traces of PVA80 for the first and second heating runs (heating rate, 10 °C/min).

$F(T)$ values means a higher crystallization rate. However, the physical significance of $a=n/m$ is less obvious, and further insight is needed.

3.3. Thermal transitions of PVA80

On heating, PVA undergoes glass, structural, and melting transitions, and eventually decomposes at elevated temperatures. The thermal properties of this polymer are of considerable interest because of their influence on processing and applications, as mentioned in the introduction session. The same is true for PVA80.

Fig. 8 shows the DSC thermograms of PVA80 for the first and second heating runs. The glass transition temperature is about 50 °C in the raw PVA80 sample. The melting temperature of the raw PVA80 sample is around 180 °C, with the melting peak starting from 150 °C (first heating). From the second heating run, however, one can see that the melting peak starts from 110 °C and ends around 185 °C, i.e. PVA80 crystals formed from the melt crystallization has a broad melting temperature range. It also can be seen from the second heating run that the glass transition temperature, T_g, changes to 70 °C. The T_g of PVA80 was increased about 20 °C after the melt crystallization, primarily due to the promoted hydrogen bonding interactions between the vinyl acetate groups and the hydroxyl groups, as discussed below. Of course, the evaporation of water on the first run may also contribute in some degree to the increase in T_g of the sample.

In addition to differential scanning calorimetry (DSC), FTIR is a routine method of monitoring the melting behavior of a semi-crystalline polymer, via a crystalline band. There is only one crystalline band in PVA [3], located around 1144 cm^{-1}. Although there are some discrepancies in the opinions on the possible origin of this band [3,54], e.g. whether it is a C–O stretching, C–C stretching, or H-bonded OH in the crystalline phase, the crystalline feature of this band can be easily verified by its temperature sensitivity, as shown in Fig. 9. The intensity variation of this band with temperature is more clearly shown

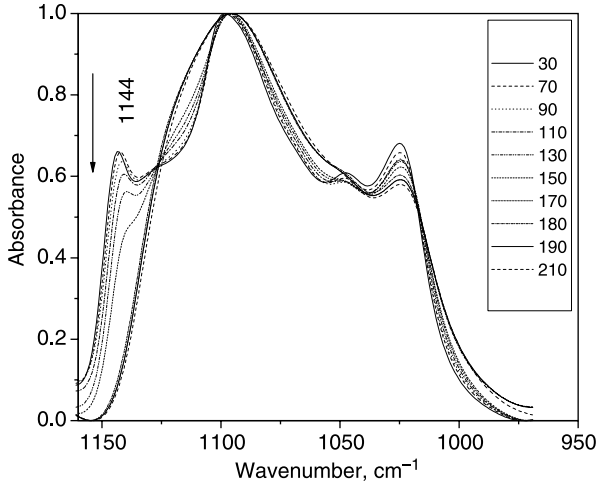

Fig. 9. Scale-expanded IR spectra of PVA80 in the region of 1160–950 cm^{-1} measured from 30 to 210 °C.

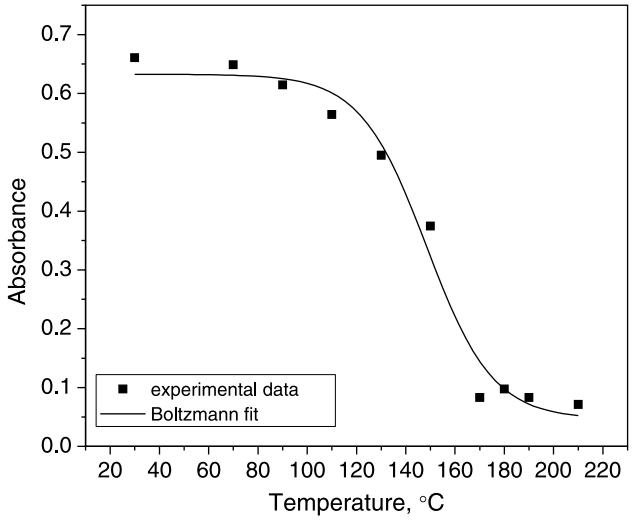

Fig. 10. Intensity variation of the crystalline band at 1144 cm^{-1} with temperature.

in Fig. 10. It is evident that, above 110 °C, the intensity of the crystalline band at 1144 cm^{-1}, decreases rapidly with increasing temperature. This trend lasts until 180 °C. Coincidentally, this is consistent with the DSC result of 2nd heating curve, shown in Fig. 8, indicating that the crystals formed from the film casting, followed by annealing at 60 and 80 °C, are similar to those from the melt crystallization in the DSC cell.

PVA80 is a partially hydrolyzed PVA. It can be regarded as a copolymer of vinyl alcohol and vinyl acetate, as depicted in

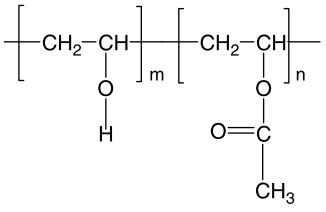

Scheme 1. Chemical structure of PVA80.

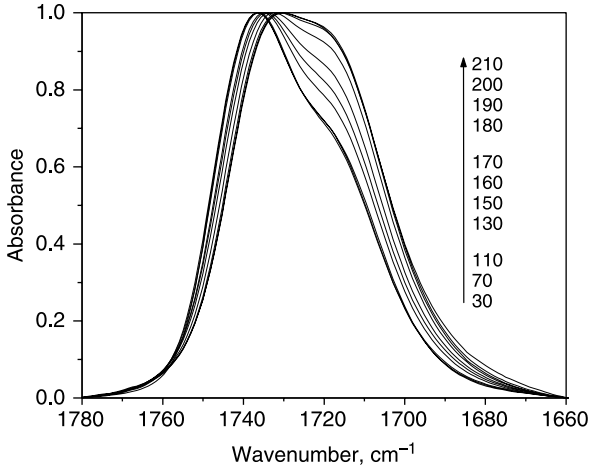

Fig. 11. Scale-expanded IR spectra of PVA80 in the C=O stretching band region collected over a range from 30 to 210 °C.

Scheme 1. Obviously, hydrogen-bonding interaction among hydroxyl groups and that between the carbonyl groups and the hydroxyl groups will be a significant feature in this polymer, while analyzing the thermal behaviors of PVA80 using FTIR.

Fig. 11 shows IR spectra (normalized to the same intensity of 'free' C=O band) of PVA80 in the C=O stretching band region collected over a temperature range from 30 to 210 °C. Three significant stages can be separated. Below 110 °C, the relative intensity of hydrogen bonded C=O band around 1715 cm^{-1} does not have a measurable change. A dramatic increase in the relative intensity of hydrogen bonded C=O band around 1715 cm^{-1} starts from 110 °C, and this trend lasts until 180 °C. Above 180 °C, the relative intensity of hydrogen bonded C=O band around 1710 cm^{-1} does not change much again. These three stages are more clearly demonstrated in Fig. 12. Rich information can be revealed from the above observations.

On the first stage, below 110 °C, the relative intensity of hydrogen bonded C=O band around 1715 cm^{-1} does not have

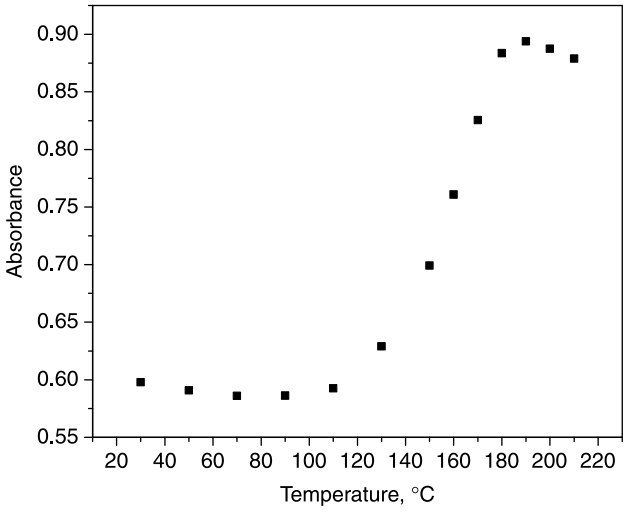

Fig. 12. Relative intensity variation of hydrogen bonded C=O band around 1715 cm^{-1} with temperature.

a measurable change. This might be beyond one's expectation. The glass transition temperature of raw PVA80 material is about 50 °C, as shown on the first heating curve in Fig. 8. After the melt crystallization, the T_g of PVA80 is around 70 °C, primarily due to the promoted hydrogen bonding interactions between the carbonyl groups and the hydroxyl groups of PVA80 (more on this below). Based on the general effect of temperature on hydrogen bonding in amorphous polymers and blends [55], above the T_g, the relative intensity of hydrogen bonded C=O band around 1715 cm^{-1} should be decreasing with increasing temperature, due to the breaking and weakening of hydrogen bonds with increasing temperature, which can be verified by a continuous higher wavenumber shift of the OH stretching band in the region of 3800–3100 cm^{-1} from 30 to 210 °C (Fig. 13). But, the question is, why the OH stretching band in the region of 3800–3100 cm^{-1} continuously shifts to a higher wavenumber from 30 to 110 °C, while the relative intensity of hydrogen bonded C=O band around 1710 cm^{-1} does not have a measurable change below 110 °C? We will come back to this later.

The significant increase in the relative intensity of hydrogen bonded C=O band around 1715 cm^{-1} on the second stage, i.e. from 110 to 180 °C reveals another counter-intuitive phenomenon, in terms of the general effect of temperature on the relative intensity of hydrogen bonded C=O band.

The above counter-intuitive phenomenon on the second stage, however, demonstrates that hydrogen bonding interaction between OH and C=O groups of PVA80 is largely promoted from 110 to 180 °C. This result will become straightforward if one recalls the semicrystalline feature of PVA80 and takes a look at the 2nd heating curve of PVA80 in Fig. 8, i.e. PVA80 crystals formed from the melt crystallization under this experimental condition starts to melt at 110 °C and ends at 180 °C. Coincidently, this is a perfect match with the temperature range where the relative intensity of hydrogen bonded C=O band around 1715 cm^{-1} increases significantly in the IR experiment (Figs. 11 and 12). This indicates that the melting of crystalline phase and the breaking, as well as

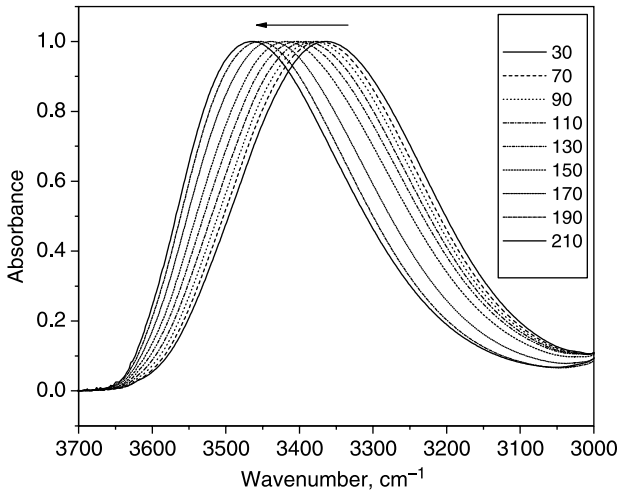

Fig. 13. Scale-expanded infrared spectra of PVA80 in the range of 3700–3000 cm^{-1} taken at different temperatures (°C).

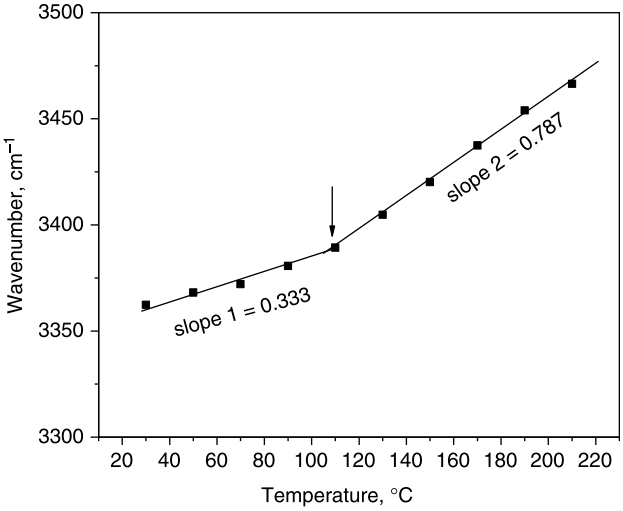

Fig. 14. Peak shift of OH stretching band in the region of 3800–3100 cm^{-1} with temperature.

weakening with increasing temperature of hydrogen bonds among hydroxyl groups in the crystalline phase give rise to the significant increase in the relative intensity of hydrogen bonded C=O band around 1715 cm^{-1}. This, in turn, implies that peak shift of OH stretching band in the region of 3800–3100 cm^{-1} below 110 °C (Fig. 13) must arise largely from the relaxation of O-H bond in the amorphous state of PVA80. This speculation can be fairly verified by the relatively low peak shifting rate below 110 °C, compared to that above 110 °C, as shown in Fig. 14. The peak-shifting rate above 110 °C is two times larger than that below 110 °C. It is probable that the hydroxyl groups in the amorphous state of PVA80 do not gain enough mobility when the temperature is increased from 30 to 110 °C to hydrogen bond with extra 'free' C=O groups available, due to the steric hindrance of non-melted crystallites. This might be the reason that we observed peak shift of OH stretching band in the region of 3800–3100 cm^{-1} below 110 °C, but we did not see a measurable increase of the relative intensity of hydrogen bonded C=O band around 1715 cm^{-1}.

It turns out that the higher wavenumber shift of the OH stretching band does not necessarily verify the promoted formation of hydrogen bonds between OH and C=O groups. This is naturally true, because even without the formation of hydrogen bonds between OH and C=O groups, increasing temperature alone will also lead to the peak shift of OH stretching band to a higher wavenumber. So, the higher wavenumber shift of the OH stretching band above 110 °C shown in Fig. 13 is a combination of hydrogen bond formation between OH and C=O groups of PVA80 and weakening of hydrogen bond with increasing temperature.

It is very interesting to notice that the intensity variation with temperature of hydrogen-bonded C=O band around 1715 cm^{-1} (Figs. 11 and 12) is the mirror image of that of the crystalline peak at 1144 cm^{-1} (Figs. 9 and 10), i.e. the intensity of the crystalline band at 1144 cm^{-1}decreases, while that of the hydrogen-bonded C=O band around 1715 cm^{-1} increases with increasing temperature above 110 °C. And this

trend lasts until 180 °C. This demonstrates that the melting behavior of PVA80 can be probed via a non-crystalline hydrogen-bonded C=O band using FTIR. This is, of course, an unique result.

As shown in Fig. 8, for a melt-crystallized PVA80 sample under non-isothermal condition, it has an extremely broad melting temperature range, from 110 to 180 °C. Melting peak broadening was already revealed in VAc/VOH copolymers [56], where the mole percent of VAc is about 0.75–6.81. Due to the much lower content of VAc units in the PVA copolymer, the melting peak broadening is, of course, not as significant as in PVA80 studied here. This indicates that the incorporation of VAc units has great effect on the crystallization of VOH units. It is well known that, the profile of the DSC melting peak corresponds to the distribution of the lamellar thickness. This means that the extremely broad melting peak of PVA80 is a result of broad distribution of its lamellar thickness. In other words, the incorporation of VAc units largely broadens the distribution of PVA lamellar thickness.

4. Conclusions

In this report, the non-isothermal crystallization behavior and thermal transitions of PVA80, a poly(vinyl alcohol) with 80% degree of saponification, has been studied using differential scanning calorimetry (DSC) and FTIR.

The possible sample degradation of PVA80 under non-isothermal crytallization was first looked into, because it has been an important issue associated with the crystallization of a fully hydrolyzed PVA. But no significant degradation or dehydration of PVA80 was detected using FTIR and DSC.

Ozawa equation and the Mo method of combining Ozawa and Avrami equations have been applied to analyze the non-isothermal crystallization of PVA80. The temperature range, over which the Ozawa equation can be applied, is in a narrow range from 80 to 100 °C, though it does not work in the whole temperature range investigated. Neither the secondary crystallization nor the quasi-isothermal nature of the treatment is the reason for the deviation from the Ozawa equation. It only results from the large relative difference in the values of the relative crystallinity X_t under different cooling rates, which is a matter of cooling rate dependent crystallization. The combination of the Ozawa and Avrami equations was successful in describing the non-isothermal crystallization of PVA80 in the whole temperature range investigated. The isoconversional method developed by Friedman was attempted to estimate the activation energy for this non-isothermal crystallization, but failed, because the variation of temperature T to arrive at a certain value of X_t under different cooling rates may not be a monotonic change with cooling rate.

PVA80 undergoes glass, structural, and melting transitions upon heating from RT to 210 °C, and hydrogen-bonding interactions play a key role in the thermal transitions of PVA80, which makes it possible to monitor the melting behavior of PVA80 via a non-crystalline hydrogen-bonded C=O band using FTIR. When temperature was increased from RT to 110 °C, the hydrogen-bonded C=O band does not have measurable change. From 110 to 180 °C, the intensity of the hydrogen-bonded C=O band increases due to the promoted hydrogen-bonding interactions between the C=O groups in the amorphous phase and the hydroxyl groups from the crystalline phase, which is the result of melting of crystallites. The glass transition temperature of PVA80 was raised about 20 °C, after the sample was melt-crystallized, also primarily due to the promoted hydrogen bonding interactions between the vinyl acetate and vinyl alcohol units. The melt-crystallized PVA80 sample, has a broad melting temperature range measured by DSC, which is consistent with the FTIR result of a casting film, followed by annealing at 60 and 80 °C.

Acknowledgements

H. H. thanks JSPS (the Japan Society for the Promotion of Science) for financial support. This work was partially supported by ‘Open Research Center’ project for private universities: matching fund subsidy from MEXT (Ministry of Education, Culture, Sports, Science and Technology), 2001–2005. This work was also supported by Kwansei-Gakuin University ‘Special Research’ project, 2004–2008.

References

[1] Pritchard J, editor. Poly(vinyl alcohol): basic properties and uses. London: MacDonald Technical and Scientific; 1970.
[2] Finch CA, editor. Poly(vinyl alcohol)-properties and applications. London: Wiley; 1973.
[3] Finch CA, editor. Poly(vinyl alcohol)-developments. London: Wiley; 1992.
[4] Jang J, Lee DK. Polymer 2003;44:8139.
[5] Bunn CW, Peiser HS. Nature 1947;159:161–2.
[6] Bunn CW. Nature 1948;161:929–30.
[7] Ricciardi R, Gaillet C, Ducouret G, Lafuma F, Laupretre F. Polymer 2003;44:3375–80.
[8] Vigolo B, Penicaud A, Coulon C, Sauder C, Pailler R, Journet C, et al. Science 2000;290:1331–4.
[9] Launois P, Marucci A, Vigolo B, Bernier P, Derre A, Poulin P. J Nanosci Nanotechnol 2001;2:125–8.
[10] Vigolo B, Poulin P, Lucas M, Launois P, Bernier P. Appl Phys Lett 2002; 81:1210–2.
[11] Poulin P, Vigolo B, Launois P. Carbon 2002;40:1741–9.
[12] Dalton AB, Collins S, Munoz E, Razal JM, Ebron VH, Ferraris JP, et al. Nature 2003;423:703.
[13] Suzuki T, Ichihara Y, Yamada M, Tonomura K. Agric Biol Chem 1973; 37:747.
[14] Chiellini E, Corti A, D’Antone S, Solaro R. Prog Polym Sci 2003;28:963.
[15] Azuma Y, Yoshie N, Sakurai M, Inoue Y, Chujio R. Polymer 1992;33: 4763.
[16] Yoshie N, Azuma Y, Sakurai M, Inoue Y. J Appl Polym Sci 1995;56:17.
[17] Ikejima T, Yoshie N, Inoue Y. Macromol Chem Phys 1996;197:869.
[18] Ikejima T, Cao A, Yoshie N, Azuma Y, Inoue Y. Polym Degrad Stab 1998;62:463.
[19] Ikejima T, Inoue Y. Macromol Chem Phys 2000;201:1598.
[20] Zhao L, Tsuchiya K, Inoue Y. Macromol Biosci 2004;4:699.
[21] Huang H, Hu Y, Zhang JM, Sato H, Zhang HT, Noda I, et al. J Phys Chem 2005;109:19175–83.
[22] Medellin-Rodriguez FJ, Phillips PJ, Lin JS. Macromolecules 1996;29: 7491.
[23] Di Lorenzo ML, Silvestre C. Prog Polym Sci 1999;24:917.
[24] Long Y, Shanks RA, Stachurski ZH. Prog Polym Sci 1995;20:651.

[25] Mandelkern L. Crystallization of polymers, vol. 1. Cambridge: Cambridge University Press; 2002 [vol. 2, 2004].
[26] Ghosh AK, Woo EM, Sun YS, Lee LT, Wu MC. Macromolecules 2005; 38:4780.
[27] Barham PJ, Keller A, Otun EL. J Mater Sci 1984;19:2781.
[28] Mitomo H, Barham PJ, Keller A. Polym J 1987;19:1241.
[29] Organ SJ, Barham PJ. Polymer 1993;34:2169.
[30] Hocking PJ, Revol JF, Marchessault RH. Macromolecules 1996;29: 2467.
[31] Nobes GAR, Marchessault RH, Chanzy H, Briese BH, Jendrossek D. Macromolecules 1996;29:8330.
[32] Lambeek G, Vorenkamp EJ, Schouten AJ. Macromolecules 1995;28: 2023.
[33] Marchessault RH, Kawada J. Macromolecules 2004;37:7418.
[34] Probst O, Moore EM, Resasco DE, Grady EP. Polymer 2004;45:4437.
[35] Yamaura K, Kumakura R. J Appl Polym Sci 2000;77:2872.
[36] Dai LX, Yu SY. Polym Adv Technol 2003;14:449.
[37] Peppas NA, Hansen PJ. J Appl Polym Sci 1982;27:4787.
[38] Endo R, Amiya S, Hikosaka M. J Macromol Sci, Part B: Phys 2003;B42: 793.
[39] Kissinger HE. J Res Natl Bur Stand 1956;57:217.
[40] An YX, Dong LS, Mo ZS, Liu TX, Feng ZL. J Polym Sci, Polym Phys 1998;36:1305.
[41] Vyazovkin S. Macromol Rapid Commun 2002;23:771.
[42] Friedman HL. J Polym Sci C 1966;6:143.
[43] Vyazovkin S. J Comput Chem 1997;18:393.
[44] Vyazovkin S. J Comput Chem 2001;22:178.
[45] Vyazovkin S, Sbirrazzuoli N. Macromol Rapid Commun 2002;23:766.
[46] Ren MQ, Song JB, Zhao QX, Li YS, Chen QY, Zhang HF, et al. Polym Int 2004;53:1658.
[47] Liu TX, Mo ZS, Wang SE, Zhang HF. Polym Eng Sci 1997;37:568.
[48] Lopez LC, Wilkens GL. Polymer 1989;30:882.
[49] Ozawa T. Polymer 1971;12:150.
[50] Cebe P, Hong SD. Polymer 1986;27:1183.
[51] Eder M, Wlochowic A. Polymer 1983;24:1593.
[52] Liu JP, Mo ZS, Qi YC, Zhang HF, Chen DL. Acta Polym Sinica 1993;1:1.
[53] Ren MQ, Chen QY, Song JB, Zhang HL, Sun XH, Mo ZS, et al. J Polym Sci Polym Phys 2005;43:553.
[54] Fujii K. J Polym Sci 1972;D1:431.
[55] Coleman MM, Graf J, Painter PC. Specific interactions and the miscibility of polymer blends. PA, USA: Technomic, Lancaster; 1991.
[56] Tubbs RK. J Polym Sci A 1965;3:4181.